Published in final edited form as:
Neurobiol Aging. 2014 July ; 35(7): 1755–1768. doi:10.1016/j.neurobiolaging.2014.01.008.

Accelerated Aging of Selective Brain Structures in HIV Infection: A Controlled, Longitudinal MRI Study

Adolf Pfefferbaum[1,2], **David A. Rogosa**[3], **Margaret J. Rosenbloom**[2], **Weiwei Chu**[1], **Stephanie A. Sassoon**[1], **Carol A. Kemper**[4,5], **Stanley Deresinski**[4,5], **Torsten Rohlfing**[1], **Natalie M. Zahr**[1,2], and **Edith V. Sullivan**[*,2]

[1]Neuroscience Program, SRI International, Menlo Park, CA

[2]Department of Psychiatry & Behavioral Sciences, Stanford University School of Medicine, Stanford, CA

[3]Departments of Education and Biostatistics, Stanford University, Stanford, CA

[4]Division of Infectious Diseases, Santa Clara Valley Medical Center, Santa Clara, CA

[5]Department of Medicine, Stanford University School of Medicine, Stanford, CA

Abstract

Advances in treatment have transformed HIV infection from an inexorable march to severe morbidity and premature death to a manageable chronic condition, often marked by good health. Thus, infected individuals are living long enough that there is a potential for interaction with normal senescence effects on various organ systems including the brain. To examine this interaction, the brains of 51 individuals with HIV infection and 65 uninfected controls were studied using 351 MRIs and a battery of neuropsychological tests collected two or more times over follow-up periods ranging from 6 months to 8 years. Brain tissue regions of interest showed expected age-related decrease in volume; CSF-filled spaces showed increase in volume for both groups. Although HIV infected individuals were in good general health, and free of clinically-detectable dementia, several brain regions supporting higher-order cognition and integration of functions showed acceleration of the normal aging trajectory, including neocortex, which extended from the frontal and temporal poles to the parietal lobe, and the thalamus. Beyond an anticipated increase in lateral ventricle and Sylvian fissure volumes and decrease in tissue volumes (specifically, the frontal and sensorimotor neocortices, thalamus, and hippocampus) with longer duration of illness, most regions also showed accelerated disease progression. This accelerated loss of cortical tissue may represent a risk factor for premature cognitive and motor compromise if not dementia. On a more promising note, HIV-infected patients with increasing CD4 counts exhibited slower expansion of Sylvian fissure volume and slower declines of frontal and temporoparietal cortices, insula, and hippocampus tissue volumes. Thus, attenuated shrinkage of these brain regions, likely with adequate pharmacological treatment and control of further infection, has the potential of abating decline in associated, higher-order functions, notably, explicit memory, executive functions, self-regulation, and visuospatial abilities.

[*]**Correspondence**: Edith V. Sullivan, Ph.D., Department of Psychiatry and Behavioral Sciences, Stanford University School of Medicine (MC5723), 401 Quarry Road, Stanford, CA 94305-5723, phone: (650) 859-2880, FAX: (650) 859-2743, edie@stanford.edu.

Keywords

cortex; MRI; HIV; AIDS; ventricles; brain structure; longitudinal

Introduction

Advances in antiretroviral treatment have transformed infection with the human immunodeficiency virus (HIV) and its sequelae, acquired immune deficiency syndrome (AIDS), from an inexorable march to severe morbidity and premature death to a manageable chronic condition, often marked by good health (Aberg, et al., 2009, Justice, 2010, Holt, et al., 2012). Young adults infected early in the epidemic age, however, face the cognitive and health challenges of normal aging burdened by the somatic, neurological, and neuropsychological consequences of HIV/AIDS. One projection indicates that by 2015, more than half of HIV-infected individuals will be at least 50 years old (Luther and Wilkin, 2007). In addition, this cohort of long-infected, 50+ year old HIV/AIDS patients is now being supplemented by a wave of newly infected elders (for sources, see Karpiak, 2011), with the incidence of first infections after age 50 now accounting for 17% of new HIV/AIDS diagnoses (The AIDS Institute National HIV/AIDS and Aging Awareness Day Fact Sheet). Older individuals newly acquiring HIV infection are typically less likely than younger ones to seek treatment early and thus initially present with lower CD4 counts and higher incidence of AIDS-defining events than those under age 50 (Althoff, et al., 2010). Although antiretroviral treatment (ART) regimens have allowed many HIV-infected individuals to maintain normal lives, increasing evidence indicates that the early viral assault, reflected in depleted CD4 counts (nadir CD4), leaves a persistent stigma on the brain (Jernigan, et al., 2011, Pfefferbaum, et al., 2012) and residual cognitive deficits (Valcour, et al., 2006) even when current viral load remains suppressed and CD4 counts rise to healthy levels (Heaton, et al., 2011).

More than two decades of cross-sectional MRI studies of HIV-infected groups have revealed structural volume deficits in various brain regions and tissue types relative to controls. Initial reports identified striatal volume deficits (Aylward, et al., 1993). Early in the ART era, white matter volume deficits and ventricular and sulcal enlargement were observed (Stout, et al., 1998), although greater gray than white matter volume deficits accompanied advanced CDC symptom stage (Di Sclafani, et al., 1997). Local cortical thinning, particularly frontal and temporal, was related to low CD4 cell count (Thompson, et al., 2005) and high peripheral mononuclear cell load (Kallianpur, et al., 2011). Although cognition has been shown to benefit from antiretroviral therapies (cf., Heaton, et al., 2011), there is evidence for potential neurotoxicity of long-term use of these potent pharmacotherapies (Letendre, et al., 2008, Becker, et al., 2011b, Ances, et al., 2012). Brain structure-function relations are also reported, where poorer performance on cognitive or motor tests correlated with smaller regional brain volumes (Thompson, et al., 2005, Pfefferbaum, et al., 2006, Castelo, et al., 2007, Paul, et al., 2008, Becker, et al., 2011a, Kuper, et al., 2011, Sullivan, et al., 2011b). HIV-infected adults who had experienced an AIDS-defining event had thinner primary sensory, motor, and premotor cortices (Thompson, et al., 2005), smaller cortical volumes, larger total ventricular size (Cohen, et al., 2010), and smaller corpora callosa (Pfefferbaum, et al., 2006, Thompson, et al., 2006). Further, HIV disease-related factors associated with greater volume abnormalities included CD4 cell-count nadir, clinical staging, history of AIDS-defining events, infection age, and current age (Pfefferbaum, et al., 2012).

Platelet decline across biannual examination in seropositive patients age 50 years and older was predictive of extent of gray matter volume deficits (but not measures of white matter or CSF volumes) observed at a single MRI; curiously, greater CSF volumes correlated with

higher CD4 counts (Ragin, et al., 2011). Another cross-sectional MRI study of 251 HIV-infected individuals reported that lower nadir CD4 cell counts, *higher* current CD4 cell counts, detectable viral load, HCV infection, and longer ART exposure all predicted white matter and CSF volume abnormalities (Jernigan, et al., 2011). Our finding that age at HIV infection was a significant unique predictor of smaller anterior cingulate volumes suggests a greater vulnerability of an older brain to the deleterious effects of the disease (Pfefferbaum, et al., 2012).

Cross-sectional studies have been instrumental in identifying brain regions and systems that are affected in HIV infection and factors that might contribute to enhanced effects but remain limited to speculation about the potential interaction of these effects with aging and variables that change with disease progression or mitigation (e.g.,Ances, et al., 2012). An MR spectroscopy study reported local differences in brain-disease variable relations, where abnormally low metabolite levels of N-acetylaspartate (NAA), a marker of neuronal integrity, showed accelerated decline with age in the frontal white matter but not in other areas of the brain sampled. By contrast, lower NAA occurred in the caudate nucleus with longer disease duration, suggesting local differences in vulnerability to disease variables in an aging context (also see Chang, et al., 2013, Cysique, et al., 2013). Although older HIV-infected men and women can exhibit greater brain structural volume deficits or functional abnormalities, identified with resting state functional MRI (rs-fMRI), than their younger counterparts, absence of an age-HIV infection interaction failed to support exacerbation of the consequences of infection with age for either volumetric measures (Ances, et al., 2012) or connectivity measures (Thomas, et al., 2013). In contrast with these rs-fMRI and volumetric findings but in concert with the MRS results, a task-activated fMRI study observed an age-HIV infection interactio locally in the attention network in cognitively intact HIV-infected individuals but compromised in an HIV-infected group with cognitive impairment. Absence of an age-HIV infection interaction was also noted in a study using MR diffusion tensor imaging to measure the integrity of local white matter microstructure (Nir, et al., 2013), although another DTI study identified age and presence of the E4 allele geneotype as risk factors for greater abnormalities in local white matter integrity (Jahanshad, et al., 2012). The inconsistency of these findings may be, at least in part, attributable to the cross-sectional examination of a dynamic disease. Indeed, any conclusion determining whether aging interacts and exacerbates the untoward effects of HIV infection, or alternatively, whether disease progression is a greater contributor than age to decline requires longitudinal study of the relevant variables in HIV infected groups (cf., Holt, et al., 2012, Spudich and Ances, 2012).

The few published longitudinal volumetric MRI studies have been conducted over relatively brief intervals, typically one to two years. The initial study found faster rate of cortical volume decline in mild (CDC stage A) and severe (CDC stage C) stages of HIV infection relative to changes observed in infection-free controls and faster rates of white matter volume decline in the HIV-infected subgroup with stage C than stage A severity level. Further, decline in caudate nucleus volume and increase in ventricular volume were greater in the HIV-infected group that progressed from a less severe to a more severe CDC stage across MRI sessions, and these changes in brain volumes correlated with decline in CD4 cell count (Stout, et al., 1998). A 2-year longitudinal study indicated widespread white matter volume loss or posterior gray matter loss (parietal, occipital, and cerebellar) in virally-suppressed HIV individuals, depending on analysis approach; those without complete viral suppression exhibited accelerated volume loss in gray and white matter compared with declines measured in controls (Cardenas, et al., 2009). Examination of HIV-infected individuals before and about 6 months after starting highly active antiretroviral treatment (HAART) revealed improvement in neuropsychological test performance but no appreciable

change in regional brain volumes (Ances, et al., 2012). Furthermore, in this study, older age at MRI and age at HIV infection were each independently related to smaller brain volumes.

Given that the aging brain is increasingly vulnerable to endogenous and exogenous insult, we expected that HIV infection would interact with normal aging to produce accelerated cortical volume decline and CSF volume increase relative to changes known from longitudinal study to occur in normal aging (e.g., Resnick, et al., 2003, Driscoll, et al., 2009, Raz, et al., 2010, Taki, et al., 2011, Pfefferbaum, et al., 2013). The potential of accelerated cortical volume loss would put HIV-infected individuals at heightened risk for cognitive compromise and dementia. Thus, the principal aim of this longitudinal neuroimaging study was to identify interactions between brain insults such as HIV-related regional tissue volume decline or ventricular or sulcal expansion and aging that increase susceptibility to premature functional decline. Further aims were to identify HIV-related factors, including age at onset of infection, duration of infection, and CNS penetration burden of HIV medications, that are significant correlates of regional brain structural volume changes, and to examine whether and when over the course of HIV infection brain volume changes contribute to deterioration in clinical, cognitive, and motor abilities over and above that expected with normal aging.

Material and methods

Participants

A total of 351 MRIs were included in this analysis: 187 in the control group and 164 in HIV group. To be included in this longitudinal analysis, participants were required to have two or more MRI data sets that could be quantified with our longitudinal, atlas-based parcellation method (Sullivan, et al., 2011a, Pfefferbaum, et al., 2013). The participants were drawn from our ongoing longitudinal study; cross-sectional analysis of baseline MRI data was reported previously (Pfefferbaum, et al., 2006, Pfefferbaum, et al., 2012). The HIV-infected group was chosen to be free of a history of alcohol use disorder. A control group was selected to match the age range of the HIV-infected group at baseline: 19.6 to 67.6 years. Of the 108 controls and 59 HIV-infected individuals reported in the baseline study, 116 men and women had at least two analyzable MRI studies: 51 with HIV infection and 65 uninfected controls. Of these, 38 patients and 34 controls had 3 MRIs; 19 patients and 16 controls had 4 MRIs; and 10 patients and 7 controls had 5 MRIs (Figure 1; Table 1). The mean±SD time between first and last MRI was 3.10±2.18 years (range=0.56 to 8.24 years) for controls and for HIV-infected group 4.01±2.62 years (range=0.74 to 8.93 years).

Recruitment—Following our laboratory protocol previously described (Pfefferbaum, et al., 2006, Pfefferbaum, et al., 2012), patients were recruited by referral from local outpatient HIV/AIDS treatment centers, presentations by project staff, and distribution of flyers at community events. Control participants were recruited by referral from patient participants, Internet posting, flyers, and word of mouth. Brief screening identified exclusionary factors — history of schizophrenia, bipolar disorder, current or past alcohol abuse or dependence, neurological disease not related to alcohol use or HIV, or inability to undergo MRI. Those meeting initial inclusion criteria were invited for a detailed assessment at our laboratory or the AIDS Community Research Consortium (ACRC), where trained medical research staff informed them about the full scope of the study and obtained written informed consent. Only HIV-infected participants with CD4 cell count >100/mm^3 and Karnofsky score (Karnofsky, 1949) >70 (can care for self but unable to carry out normal activity) were considered for study enrollment.

Clinical evaluation—Calibrated research clinical psychologists or a research nurse conducted a Structured Clinical Interview for DSM-IV (First, et al., 1998) to exclude

individuals who met lifetime criteria for schizophrenia or bipolar disorder; to identify volunteers meeting criteria for depressive or anxiety disorder; and to confirm that prospective controls did not meet DSM-IV criteria for any Axis I disorder, including alcohol or other substance use or abuse disorders and to identify and characterized drug abuse or dependence in participants with HIV infection. All participants were tested for HIV status and hepatitis C; additional blood tests characterized viral load and CD4 cell count in HIV-positive participants.

No participant met DSM-IV criteria for lifetime alcohol dependence or abuse. Of the 51 HIV infected participants, 17 (33.3%) had a lifetime history of DSM-IV drug abuse or dependence at baseline. For those with drug history, mean length of remission (i.e., time since last met DSM-IV criteria for drug abuse/dependence) was 526.0 ± 428.4 weeks. The range of those with drug dependence was 68 to 1320 weeks; one man met criteria for drug abuse with a 7-week remission before initial study. With this exception, no other participant met DSM-IV criteria for drug abuse or dependence within the year prior to their baseline visit; the median length of time since last met criteria for drug abuse or dependence was 442 weeks. The most common drug of abuse was cocaine, reported by 15/17 of those with drug history, followed by amphetamine and opiates, each reported by 6/17 of those with drug history.

Group characteristics (Table 2)—The groups were matched on age and were similar in sex distribution, handedness (Crovitz and Zener, 1962), and body mass index (BMI). Relative to the control group, the HIV-infected group had fewer years of education, lower estimated intelligence scores (National Adult Reading Test (Nelson, 1982)), lower socioeconomic status (Hollingshead and Redlich, 1958), more depressive symptoms (Beck, et al., 1996), lower Global Assessment of Functioning scores (First, et al., 1998), and were more likely to have been cigarette smokers.

HIV-related health indices measured at the baseline MRI appear in Table 2 and include self-estimated age at HIV infection, HIV infection duration, CD4 cell count, CD4 nadir, viral load, and incidence of hepatitis C viral infection. At baseline, 25 of the 51 HIV-infected participants had had an AIDS-defining event (CD4 cell count below 100/mm^3 or symptoms indicative of AIDS). At baseline, 80% (41/51) of HIV-infected participants were on HAART medications. The median length of time on HAART was 18 months (range = 1 week to 187 months; mean±SD = 35.5±43.8 months). To quantify the potential effect of antiretroviral medication regimen reported at study entry, we calculated the CNS penetration effectiveness (CPE) index (Letendre, et al., 2010). Mean CPE score was 8.5 (median = 8.0, range = 5 to 18). No patient was clinically demented at baseline, none showed evidence of opportunistic infections, and Karnofsky score indicated intact performance on activities of daily living (range across all MRI sessions = 80 to 100).

MRI acquisition and quantification

Acquisition parameters—All MRI data were collected on a GE 1.5T Signa Twin whole-body system with a quadrature head coil (General Electric Healthcare, Waukesha, WI). Two coronal structural sequences were used for the analysis: a SPoiled Gradient Recalled (SPGR) echo sequence (TR=25 ms, TE=5 ms, flip angle=30°, matrix=256×192, FOV=24 cm, thick=2 mm, skip=0 mm, 94 slices) and a dual-echo fast spin echo (FSE) sequence (TR=7500 ms, TE1/2=13.5/108.3 ms, matrix = 256×192, FOV=24 cm, thick=4 mm, skip=0 mm, 47 slices). The imaging parameters for this longitudinal study were established 10 years ago and maintained throughout the study. For further assurance of consistency over the study period, we have complete control over the acquisition protocols for our MRI studies. Even though this study extended over a considerable period of time, we used the same

acquisition protocol and ran phantoms before and after equipment upgrades to examine drift. Routine phantom data were used to evaluate spatial fidelity, and drift was corrected by adjusting scanner calibration parameters when necessary to maintain spatial stability within manufacturer guidelines.

SRI24 atlas-based parcellation—MRI quantification details have been described previously (Pfefferbaum, et al., 2012, Pfefferbaum, et al., 2013) and are summarized here. All structural images were first corrected for intensity inhomogeneity by applying a second-order polynomial, multiplicative bias field computed via entropy minimization (Likar, et al., 2001). The late-echo FSE image was corrected using the bias field computed from the corresponding early-echo image to maintain the ratio of early- and late-echo values at each pixel. For each participant and each session, the bias-corrected early-echo FSE image was then registered to the bias-corrected SPGR image using intensity-based nonrigid image registration (Rohlfing and Maurer, 2003) (http://nitrc.org/projects/cmtk). The SPGR, early-echo FSE, and late-echo FSE images were each skull stripped using FSL's Brain Extraction Tool, BET (Smith, 2002). The early-echo and late-echo brain masks were reformatted into SPGR image space and combined with the SPGR-derived brain mask via label voting (Rohlfing and Maurer, 2005) to form the final SPGR brain mask.

The SRI24 atlas (Rohlfing, et al., 2010) (http://nitrc.org/projects/sri24) was used as the template for parcellating all brain images into regional volumes for region-of-interest- (ROI) based analysis. The SRI24 atlas was created from multi-spectral images of 24 participants, all aligned via template-free, groupwise nonrigid image registration. Structural parcellation maps were either transferred from other atlases via nonrigid registration and manually corrected, or outlined directly in the atlas, which is possible due to the clear definition of anatomical structures in the SRI24 template image as a result of the nonrigid atlas construction procedure. A complete description of the atlas construction and its validation is published elsewhere (Rohlfing, et al., 2010).

For each participant, the baseline skull-stripped SPGR images were registered to the SPGR channel of the SRI24 atlas (Rohlfing, et al., 2010) via nonrigid image registration (Rohlfing and Maurer, 2003). Cortical and subcortical parcellation maps for all participants at baseline MRI were obtained by reformatting label maps defined in SRI24 space directly into native SPGR image spaces using the participant-to-atlas coordinate transformations. Each follow-up MRI was nonrigidly registered to the baseline MRI for the same participant, and label maps were reformatted via concatenation of the follow-up-to-baseline transformation with the baseline-to-atlas transformation, thus producing longitudinally-consistent parcellations (Sullivan, et al., 2011a).

All bias-corrected and skull-stripped SPGR images were segmented into three tissue compartments (gray matter, white matter, CSF) using FSL's FAST tool (Zhang, et al., 2001). As tissue priors to both initialize and guide the classification, we used the tissue probability maps provided with the SRI24 atlas, reformatted into participant SPGR space via the same transformations described above for the atlas-based parcellation.

Regions of interest (ROIs) (Figure 2)—We quantified 11 bilateral anatomical regions: 9 tissue regions, comprising 3 neocortical (frontal comprising frontal neocortex from the pole to the central sulcus; sensorimotor cortex; and temporoparietal cortex), 2 allocortical (cingulate and insular), 4 subcortical (hippocampus, amygdala, thalamus, basal ganglia) structures, and 2 CSF-filled structures (lateral ventricles and Sylvian fissures) (Figure 2). Gray matter volume was computed for each neocortical and allocortical region, and tissue volume for each subcortical region. All regions were derived from the SRI24 SPGR template and reformatted into participant image space. The choice of quantifying these ROIs

was determined by the desire to include regions known to be affected by HIV infection and putative substrates of the neuropsychological domains measured by the composite scores, described next.

Neuropsychological testing

Testing assessed five cognitive and motor functional domains, listed next with specific tests comprising that domain noted parenthetically: Verbal/Language (National Adult Reading Test [NART] or Peabody Picture Vocabulary Test; FAS fluency), Executive Functioning (Wechsler Memory Scale-Revised [WMS-R] Attention Index; MicroCog Digit Span; Stroop Color-Word Test; Trails B or Color Trails II), Learning/Memory (WMS-R Verbal Memory Index; MicroCog Memory subtest; Rey-Osterrieth Complex Figure Test, immediate and delayed recall), and Speed of Information Processing (Stroop Color Reading Test; Trails A or Color Trails I; Digit Symbol or Symbol Digit), Motor Skills (fine finger movement test; Grooved Pegboard Test; stand-on-one-foot ataxia test).

Domain scores were calculated as follows: first, raw scores of each test measure at each test session were transformed into standardized Z-scores based on the baseline performance of the controls, who were age-range matched to the patients; then, the mean of all available test scores comprising a domain was calculated for each participant. In addition, a Summary score was derived from the mean of the domain Z-scores and re-standardized to reflect overall performance.

Statistical analysis

Brain volumes of each region were first transformed into standardized Z-scores, which adjusted regional volumes for differences in supratentorial volume modeled from the control data (Pfefferbaum, et al., 1992, Mathalon, et al., 1993, Pfefferbaum, et al., 1994). As described previously (Pfefferbaum, et al., 2013), trajectories of individual participants were calculated using the *lmer* function for linear mixed-effects modeling in the *lme4* R statistical package [http://www.r-project.org/], and based on the approach described by Laird and Ware (Laird and Ware, 1982). The *lmer* function also allowed for testing of nested random effects; for the current analysis, the effects of age and diagnosis were tested first to identify group differences in slopes of regional brain volumes. To examine longitudinal trajectories of volume change independent of age at data acquisition, we computed the trajectory slopes of each participant for each brain region with the participant's age at acquisition entered into the model as the deviation from the mean age of the multiple MRIs available for each individual participant, which we refer to as "age-centered slope" (Rogosa, et al., 1982). For example, an individual with observations at age 58, 60, and 62 years would have −2, 0, and +2 for his age-centered scores against which the slope of a brain measure is computed. Group differences were tested one-tailed, with the general hypothesis that the HIV group would have smaller tissue volumes and larger CSF volumes than controls and that their slopes reflecting volume change over age would be steeper than those of the controls.

Similar trajectory analyses were conducted on HIV group data to test for differences in brain volume slopes related to slopes of CD4 cell count, plasma viral load, platelet count, BMI, and maximal CPE across measurements. Additional tests examined relations between brain volume slopes and age at HIV infection and duration of HIV infection, for which a "durationcentered" variable was used instead of the "age-centered" variable, and followed by examination of potential accelerated change in the HIV-infected group with older age. Relations between variables were tested with Pearson product-moment correlations (r) and, where appropriate, Spearman Rank Order (Rho) correlations. Correlations were tested one-tailed, with the general hypothesis that slopes indicating smaller tissue volumes and larger

CSF volumes would be associated with older age, greater disease burden, and poorer test performance.

Analysis of neuropsychological composite scores followed the modeling used for brain volumes.

Results

In general, for the HIV-infected patients and controls, CSF-filled spaces increased and tissue volumes decreased with advancing age for both the mean regional measures and the average trajectories of the individuals (Figure 3).

Longitudinal analysis of regional brain volume trajectories: Groups differences

The primary analysis model created growth curves or trajectories of change over age, with the general hypothesis that tissue decreases and CSF-filled spaces expand with advancing adult age. In the initial longitudinal analysis, the data for each ROI for each participant in each group (HIV-infected participants and controls) were fitted with a linear mixed-effects model using the *lmer* function in the *lme4* package of R. Specifically, the supratentorial-regressed (Zscore) volumes of each ROI were fit with a function that included each participant's mean age (*agem*), age-centered linear slope (*agecent*), and diagnosis (*dx*) with the age-centered slope as the random effect.

```
fm3r <- lmer(vol~dx*agecent+agem+(agecent|subject))
```

Outputs of interest were group differences in 1) mean volume regardless of age and 2) diagnosis-by-age-centered trajectory (i.e., slope) interactions. Significant volume effects, where HIV-infected had greater volume in CSF regions and smaller volumes in tissue regions than controls, were found in the Sylvian fissures, cingulum, insula, thalamus, and hippocampus (Table 3A). Significant slope effects, where the HIV-infected group showed greater change per year over the years of observation than the control group, were detected in the lateral ventricles, insula, and hippocampus (Table 3B; Figure 3).

Test of accelerated aging in HIV-infected participants relative to controls

To explore the possibility of greater acceleration in slope with advancing age in the HIV-infected individuals, a secondary analysis applied a general linear regression model (*lm* funciton in R) to fit the individual trajectory slopes with individual mean age and diagnosis.

```
fm3s <- lm(slope~dx*agem)
```

Significant HIV-infection and age-related acceleration was found for the three neocortical regions (frontal, sensorimotor, temporoparietal) and the thalamus (Table 3C). Trends present indicated accelerated expansion of the lateral ventricles and shrinkage of the insular cortex.

Use of standardized scores allowed comparison of the goodness of fit of the age-centered slopes of different-sized ROIs. The average residual standard errors (RSE) for the individual fits were larger for all 11 ROIs of the HIV-infected participants (mean RSE=.1936) than controls (mean RSE=.1340) ($t(10)=5.121$, $p=.00045$), indicating that the age-centered slopes were better fit for the controls than the patients. Brain volumes of the HIV-infected man with recent amphetamine abuse were within 1 S.D. of the control values for all regions measured.

Relation between brain volume trajectories and duration of HIV infection

Disease progression was modeled on self-reported estimated date of HIV infection to create a duration-of-illness metric (*daysm*). These data were modeled with *lmer* to fit the head size-

regressed volume of the ROI with a function that included each participant's mean number of infection days (over all visits) and their days-infected-centered linear slope (*dayscent*) with days-infected-centered linear slope as the random effect.

fm4d <- lmer(vol~daysm*dayscent+(dayscent|subject))

Lateral ventricle and Sylvian fissure CSF volumes increased and the volumes of the frontal and sensorimotor neocortices, thalamus, and hippocampus decreased with longer duration of illness (Table 4A). In addition, more rapid disease progression in terms of steeper volume trajectories occurred with longer duration of illness in the lateral ventricles, temporoparietal neocortex, and thalamus, indicated by significant interactions of mean days of infection by slope (Table 4B; Figure 4).

Because disease duration and age were significantly correlated (r=.42, p=.0028) and therefore confounded, we used multiple regression to estimate the independent contribution of duration-centered slopes of the volumes and mean age across MRI to each ROI slope. Of the 11 ROIs, 7 had significant multiple regression results, 5 of which indicated that disease duration but not age made a significant contribution to declining tissue slope (frontal, temporoparietal, and cingulate cortices and hippocampus) or increasing CSF slope (Sylvian fissures). Only the analysis for thalamus slopes indicated that age but not disease duration made a significant independent contribution to tissue volume decline over that of disease duration. Trends for the lateral ventricles and insula were also supportive of duration of disease over age as related to volume change (Table 4C).

Longitudinal analysis of neuropsychological test performance trajectories

The same analysis procedures applied to the brain data were applied to the neuropsychological standardized composite scores for the five functional domains (Verbal/Language, Executive Functioning, Learning/Memory, Speed of Information Processing, and Motor Skills) and the Summary composite score.

fm3r<-lmer(score~dx*agecent+agem+(agecent|subject))

Overall, the HIV-infected group performed more poorly than the controls on all composites, except for Speed of Information Processing (Table 5a; Figure 5).

Trajectory analyses indicated that the HIV-infected group declined faster than controls on the Executive Function and Summary composite scores (Table 5b).

fm3s<-lm(slope~dx*agem)

Unlike the brain structural measures, all of which demonstrated a unidirectional trajectory indicating increase in CSF and decrease in tissue volume with advancing age, some of the behavioral measures improved over age, probably with practice from repeated testing (Figure 6, top). Also unlike the brain structural measures, there was no evidence of greater rate of change (i.e., age-centered-slope over age) for HIV-infected individuals relative to controls for any domain measure.

Relation between performance domain score trajectories and duration of HIV infection

Application of the disease progression model to the performance measures revealed significant improvement over mean duration of illness (*daysm*) for the Verbal/Language, Learning/Memory, Speed of Information Processing, and Summary scores (Table 6a).

fm4d=lmer(score~daysm*dayscent+(dayscent|subject))

Improvement suggests that the HIV-infected participants showed practice effects over repeated testing. Nonetheless, neither the mixed effects model (Table 6b) nor the slope

correlation model (Table 6c) revealed significant changes in the slope of performance across the duration of disease (Figure 6, bottom). Thus, HIV-infected participants with longer disease dur not show either accelerated improvement or decline compared with those more recently infected.

Use of standardized scores allowed comparison of the goodness of fit of the age-centered slopes. The average RSEs for the individual fits were greater for 5 of the 6 composite scores of the HIV-infected participants (mean RSE=.6193) than controls (mean RSE=.4717) ($t(10)=2.6677$, $p=.0445$). The failure to find fewer significant relationships between performance score trajectories and years of observation or duration of illness than found with MRI data could be explained, in part, by greater individual variability across sessions, which were poorly modeled with linear fit of individual trajectories, for the performance than the MRI data in both groups (control: mean RSE= .4717 vs. .1340) ($t=5.4236$, $p=.0015$) (HIV: mean RSE= .6193 vs. .1936) ($t=5.999$, $p=.00075$).

Correlations between brain volume trajectories and performance trajectories

Four correlations had p-values of .05 or lower, where faster declines in tissue volumes predicted faster declines in performance: slopes of Verbal/Language correlated with slopes of the thalamus (Rho=.351, p=.0161) and hippocampus (Rho=.370, p=.0108); Motor Speed with temporoparietal slopes (Rho=.361, p=.0307); and Speed of Information Processing with sensorimotor slopes (Rho=.381, p=.0086), the only correlation meeting family-wise Bonferroni correction, which required $p \leq .009$ ($\alpha=.05$, one-tailed).

The dependent variables for brain and performance analyses were standardized scores allowing comparison of the goodness of fit of the age-centered slopes. The average RSEs for the individual fits were significantly larger for the performance than brain measures for both the controls ($t=5.07$, $p=.0009$) and the HIV-infected participants ($t=6.27$, $p=.0000$). Further, the average RSEs for the individual fits were larger for all 6 measures of the HIV-infected participants (mean RSE=.4799) than controls (mean RSE=.3751). Again, the marked variability across time in performance may have precluded detection of brain structure-function correlations.

Correlation of regional brain volume trajectories with HIV disease characteristics

There was no significant difference in slopes for any ROI for those with vs. those without a history of an AIDS-defining event or HCV co-infection. Further, there were no correlations between self-reported age at infection and the slope of any ROI. The only variable that was predictive of volume trajectory slope was the maximum CPE value over the course of the study, which negatively correlated with a more rapid decline of thalamic volume (Rho=−.42, p=.0026). The HIV-infected individual body weights were stable over the observation period, with BMI changing only .04 units per year on average, and there were no significant correlations between BMI slope and any ROI slope. Neither change in platelet count nor log viral load correlated (nonparametric) with any ROI slope.

In contrast with other HIV variables, CD4 counts, which increased on average 11.4 counts/mm^3/year (range= −255 to +278), did show a relation with MRI trajectories. CD4 changes correlated significantly with 9 ROI slopes based on parametric correlations and 5 survived nonparametric tests, including the Sylvian fissures, frontal cortex, temporoparietal cortex, insula, and hippocampus (Table 7, Figure 7), indicating that increasing CD4 counts were associated with smaller increases in volumes of CSF-filled spaces and smaller decreases in regional tissue.

Finally, multiple regression analyses estimated the independent contributions of CD4 count slope and age on ROI slopes (Table 8). The overall regression was significant for 9 ROIs. In

8 cases, CD4 slope but not age was a significant predictor of ROI slope: lateral ventricles, Sylvian fissures, the three neocortical measures, cingulum, insula and hippocampus. Only the thalamus had a greater contribution from age than CD4 count change.

Discussion

These longitudinal data provide evidence for regional cortical volume loss and CSF-filled space expansion in HIV-infected individuals at levels and rates greater than those detected in normal aging. The trajectories of volume change were measured on average over 4 years and up to 8 years in some cases. The HIV-infected group had overall larger CSF-filled volumes and smaller tissue volumes in all regions measured relative to the control group, and these abnormalities were statistically significant for the Sylvian fissures, cingulate cortex, insula, thalamus, and hippocampus. Regions showing substantial acceleration with aging in the HIV-infected group were the frontal, sensorimotor, and temporoparietal cortices and thalamus. Estimates of changes in cc/year for each ROI of the HIV-infected and control groups appear in Table 9. Evidence for accelerated aging in the HIV-infected group occurred despite relatively good health at study entry, in that no participant was clinically demented, had manifest problems with activities of daily living, or had evidence of opportunistic infections.

A number of HIV-related factors had been identified in published studies as potentially exacerbating brain structural decline. Testing for evidence of their relation to changes in brain volumes, we found no significant modulation of brain volume trajectories from self-reported age at infection, history of an AIDS-defining event, HCV co-infection, or changes in platelet count, log viral load, or BMI. Other variables, however, were significant predictors of volume trajectories. In particular, faster declines in thalamic volume were related to higher maximum CNS penetration effect of HIV medication. The most consistent and robust predictors of brain volume trajectories were CD4 count and duration of HIV infection, detailed next.

Beyond an anticipated increase in lateral ventricle and Sylvian fissure volumes and decrease in tissue volumes (specifically, the frontal and sensorimotor neocortices, thalamus, and hippocampus) with longer duration of illness, most regions showed an accelerated disease progression. Here, in all but two brain regions measured (thalamus and amygdala), greater rates of undesirable change occurred with longer time infected. Mitigating these brain structural signs of disease progression, positive trajectories of CD4 counts were predictive of slower expansion of Sylvian fissure volumes and slower declines of tissue volumes of the frontal and temporoparietal cortices, insula, and hippocampus. The opposing forces of disease duration and improvement in CD4 count are reminders of the dynamic course of HIV infection, especially in the context of effective pharmacological treatment. This dynamism could also provide an explanation for why these factors are not consistently found to be associated with brain structural measures in cross-sectional analysis. Prior studies indicate that low and declining CD4 count is a risk factor for AIDS (Heaton, et al., 2011) and cardiovascular events (e.g.,Grunfeld, et al., 2009) (for review, Deeks, 2011); yet, increasing CD4 counts with selective medications is also associated with premature loss of bone density (van Vonderen, et al., 2009). Our data suggest a positive role for increasing CD4 count in attenuating the potential untoward interaction of longer disease duration and aging on brain structure and perhaps offsetting negative effects of medication CNS penetration effects.

In general, older HIV-infected individuals carried the infection longer than younger ones. Multiple regression analysis used to parse these confounded variables indicated disease duration accounted for a significantly greater proportion of the variance than age to

declining tissue slope (frontal, temporoparietal, and cingulate cortices and hippocampus) or increasing CSF slope (Sylvian fissures), whereas age was a greater contributor than disease duration to thalamic volume decline. Similarly, CD4 count was a stronger predictor than age of volume slopes of the lateral ventricles, Sylvian fissures, the three neocortical measures, cingulum, insula and hippocampus. The multiple regression analyses do not discount aging as a critical factor in accelerated declines of tissue volumes or increases in CSF volumes but do indicate the multivariate problem in identifying risk factors of declining health in the aging HIV-infected population.

The neuropsychological test battery provided quantitative assessment of four cognitive and one motor domain and a Summary functional score, reflecting general performance level. This battery was modeled on that of the CHARTER Project to provide an objective metric for determination of the presence, severity, and domain of potential impairment characterizing the HIV group and also determination of HIV-Associated Neurocognitive Disorders (HAND) on an individual basis (Antinori, et al., 2007). Overall, the performance trajectories of this HIV-infected group were statistically significantly lower than of the controls on four of five composite domains (Verbal/Language, Executive Functioning, Learning/Memory, Motor Skills) and Summary composite score. The HIV-infected group showed faster rates of decline than controls on Executive Function and Summary composite scores but no evidence of accelerated rate of decline with aging or duration of HIV infection. This observation is consistent with previous studies, which provided evidence for neither an age-HIV infection interaction (but see Sacktor, et al., 2007, Valcour, et al., 2011, Ances, et al., 2012) nor a 'cortical' pattern of cognitive deficits in older patients (Scott, et al., 2011). Only one brain structure-function correlation was adequately robust to meet correction for multiple comparisons in the HIV group. This functional domain was Speed of Information Processing, on which faster performance declines correlated with faster declines of sensorimotor cortical volumes. Although this relation would be predicted *a priori*, that other brain volume-performance correlations were not significant might be related to differences in the goodness of fit of the trajectories, which was substantially better for the MRI data than for the highly variable performance data. In addition, change in performance might not be in lock step with change in brain structure, measured as volume declines (cf., Grady, et al., 1988), thus acting as a further mask to detection of actual brain structure-function relations. Moreover, even though the decline in Speed of Information Processing was not statistically significantly greater in the HIV-infected group than the controls, identification of this relation between lower performance scores and smaller brain volumes, even when decline is not statistically significant, may reflect a liability for functional impairment with disease progression and declining regional brain volume.

Analysis of individual cases identified that a greater number HIV cases than controls fell at or below 2 standard deviations (S.D.) on all neuropsychological domains except Speed of Information processing. This difference was evident also for the Summary score for 14 of 151 observations in the HIV infected group compared with only 1 of 184 observations in the control group ($\chi 2=14.77$, $p=.00012$). Review of these HIV-infected cases indicated that only one man (age 49 years at study entry, with HIV-infection for 3.5 years, 12 years of education) and one woman (age 53 years at study entry, with HIV-infection for 12 years, 11 years of education) achieved consistently low scores. Even these cases, however, would not be deemed demented because their abnormally low (average) scores were selective to verbal information processing (Verbal/Language, Executive Function, and Learning/Memory), leaving average Motor Skill and Speed of Information Processing scores in only the mildly affected range (−1.105 to −1.525 S.D.). The lower verbally-based scores might also be related to the low I.Q. estimated with the NART: 88 for the woman and 89 for the man. Further, neither case had ever experienced an AIDS-defining event. Their compromised cognitive condition was not consistently reflected in their MRI volumes. The ROI showing

the greatest abnormality in the HIV-infected man was the Sylvian fissures (1.47 S.D.), and in the HIV-infected woman, the brain volumes at or below 2 S.D. were the temporoparietal cortex, cingulum, insula, and amygdala.

Limitations

As this was a naturalistic study, we had no control over how many return visits each HIV participant would make. The numbers for baseline through fifth visits are summarized in Table 1. We were concerned that patients who only completed 2 visits might have been demographically or clinically different from those who completed 3, 4, or 5 visits. Analysis of variance comparing baseline measures from each group for age, years of education, SES, BMI, NART, BDI, GAF, days infected, CD4 count, CD4 count nadir, viral load, HCV status, or whether or not they were immunosuppressed revealed no significant group differences.

Conclusions

Longitudinal analysis revealed evidence for accelerated aging of selective brain regions over a 6 month to 8 year interval in a cohort of HIV-infected individuals who were, for the most part in good general health, and free of clinically-detectable dementia. This analysis indicated that the changes in brain volumes were consistent with accelerated aging, which is modeled with a continuous divergence from trajectories of normal aging. By contrast, performance slope differences between control and HIV groups are better modeled as premature aging, in that differences between the patients and the controls occurred without interactions with aging (cf., Brew, et al., 2009, Holt, et al., 2012). Brain regions showing acceleration were the neocortex, which extended from the frontal and temporal poles to the parietal lobe, and the thalamus, all regions supporting higher-order cognition and integration of functions. Accelerated cortical volume loss with advancing age puts HIV-infected individuals at heightened risk for cognitive compromise and dementia along with curtailed reserve to compensate for declining function arising from advancing age and disease progression (cf., Chang, et al., 2013). That we observed only modest relations between declines in brain tissue and performance could be attributable to the relatively general measures used in addition to noted differences in measurement variability. Other studies provide evidence that declines in brain structure and functions do not necessarily proceed in lock step. Indeed, the difference between the accelerated aging of brain structures and premature aging of cognitive and motor functions indicates asynchronous decline. Nonetheless, accelerated loss of cortical tissue in the current, nondemented HIV group remains a risk factor for premature cognitive and motor compromise if not dementia.

In addition to heralding premature neuro-senescence, these longitudinal data provide a note of hopeful news to HIV carriers who maintain and improve their CD4 counts. This HIV-infected cohort did exhibit slower expansion of Sylvian fissure volume and slower declines of tissue volumes of the frontal and temporoparietal cortices, insula, and hippocampus with increasing CD4 counts. Thus, attenuated shrinkage of these brain regions, likely with adequate pharmacological treatment and control of further infection, has the potential of abating decline in associated, higher-order functions, notably, explicit memory, executive functions, self-regulation, and visuospatial abilities.

Acknowledgments

The authors would like to thank the many research assistants who were diligent in scheduling and data collection over the years and note in particular Crystal Caldwell for her exceptional recruitment efforts and Priya Asok, M.D. for her care in collection and oversight of clinical laboratory data. This work was funded by the U.S. National Institute on Alcohol Abuse and Alcoholism (AA017347, AA005965, AA017168).

REFERENCES

Aberg JA, Kaplan JE, Libman H, Emmanuel P, Anderson JR, Stone VE, Oleske JM, Currier JS, Gallant JE. Primary care guidelines for the management of persons infected with human immunodeficiency virus: 2009 update by the HIV medicine Association of the Infectious Diseases Society of America. Clinical Infectious Diseases. 2009; 49:651–681. [PubMed: 19640227]

Althoff KN, Gebo KA, Gange SJ, Klein MB, Brooks JT, Hogg RS, Bosch RJ, Horberg MA, Saag MS, Kitahata MM, Eron JJ, Napravnik S, Rourke SB, Gill MJ, Rodriguez B, Sterling TR, Deeks SG, Martin JN, Jacobson LP, Kirk GD, Collier AC, Benson CA, Silverberg MJ, Goedert JJ, McKaig RG, Thorne J, Rachlis A, Moore RD, Justice AC. CD4 count at presentation for HIV care in the United States and Canada: are those over 50 years more likely to have a delayed presentation? AIDS Res Ther. 2010; 7:45. [PubMed: 21159161]

Ances BM, Ortega M, Vaida F, Heaps J, Paul R. Independent Effects of HIV,.Aging, and HAART on Brain Volumetric Measures. Journal of Acquired Immune Deficiency Syndromes. 2012

Antinori A, Arendt G, Becker JT, Brew BJ, Byrd DA, Cherner M, Clifford DB, Cinque P, Epstein LG, Goodkin K, Gisslen M, Grant I, Heaton RK, Joseph J, Marder K, Marra CM, McArthur JC, Nunn M, Price RW, Pulliam L, Robertson KR, Sacktor N, Valcour V, Wojna VE. Updated research nosology for HIV-associated neurocognitive disorders. Neurology. 2007; 69:1789–1799. [PubMed: 17914061]

Aylward EH, Henderer JD, McArthur JC, Brettschneider PD, Harris GJ, Barta PE, Pearlson GD. Reduced basal ganglia volume in HIV-1-associated dementia: results from quantitative neuroimaging. Neurology. 1993; 43:2099–2104. [PubMed: 8413973]

Beck, AT.; Steer, RA.; Brown, GK. Manual for the Beck Depression Inventory-II. San Antonio, TX: Psychological Corporation; 1996.

Becker JT, Maruca V, Kingsley LA, Sanders JM, Alger JR, Barker PB, Goodkin K, Martin E, Miller EN, Ragin A, Sacktor N, Selnes O. Factors affecting brain structure in men with HIV disease in the post-HAART era. Neuroradiology. 2011a

Becker JT, Sanders J, Madsen SK, Ragin A, Kingsley L, Maruca V, Cohen B, Goodkin K, Martin E, Miller EN, Sacktor N, Alger JR, Barker PB, Saharan P, Carmichael OT, Thompson PM. Subcortical brain atrophy persists even in HAART-regulated HIV disease. Brain Imaging Behav. 2011b; 5:77–85. [PubMed: 21264551]

Brew BJ, Crowe SM, Landay A, Cysique LA, Guillemin G. Neurodegeneration and ageing in the HAART era. J Neuroimmune Pharmacol. 2009; 4:163–174. [PubMed: 19067177]

Cardenas V, Meyerhoff D, Studholme C, Kornak J, Rothlind J, Lampiris H, Neuhaus J, Grant R, Chao L, Truran D, Weiner M. Evidence for ongoing brain injury in human immunodeficiency virus-positive patients treated with antiretroviral therapy. Journal of Neurovirology. 2009:1–10. [PubMed: 19462266]

Castelo JM, Courtney MG, Melrose RJ, Stern CE. Putamen hypertrophy in nondemented patients with human immunodeficiency virus infection and cognitive compromise. Arch Neurol. 2007; 64:1275–1280. [PubMed: 17846265]

Chang L, Holt JL, Yakupov R, Jiang CS, Ernst T. Lower cognitive reserve in the aging human immunodeficiency virus-infected brain. Neurobiol Aging. 2013; 34:1240–1253. [PubMed: 23158761]

Cohen RA, Harezlak J, Schifitto G, Hana G, Clark U, Gongvatana A, Paul R, Taylor M, Thompson P, Alger J, Brown M, Zhong J, Campbell T, Singer E, Daar E, McMahon D, Tso Y, Yiannoutsos CT, Navia B. Effects of nadir CD4 count and duration of human immunodeficiency virus infection on brain volumes in the highly active antiretroviral therapy era. Journal of Neurovirology. 2010; 16:25–32. [PubMed: 20113183]

Crovitz HF, Zener KA. Group test for assessing hand and eye dominance. American Journal of Psychology. 1962; 75:271–276. [PubMed: 13882420]

Cysique LA, Moffat K, Moore DM, Lane TA, Davies NW, Carr A, Brew BJ, Rae C. HIV, vascular and aging injuries in the brain of clinically stable HIV-infected adults: a (1)H MRS study. PLoS One. 2013; 8:e61738. [PubMed: 23620788]

Deeks SG. HIV infection, inflammation, immunosenescence, and aging. Annu Rev Med. 2011; 62:141–155. [PubMed: 21090961]

Di Sclafani V, Mackay RD, Meyerhoff DJ, Norman D, Weiner MW, Fein G. Brain atrophy in HIV infection is more strongly associated with CDC clinical stage than with cognitive impairment. Journal of International Neuropsychological Society. 1997; 3:276–287.

Driscoll I, Davatzikos C, An Y, Wu X, Shen D, Kraut M, Resnick SM. Longitudinal pattern of regional brain volume change differentiates normal aging from MCI. Neurology. 2009; 72:1906–1913. [PubMed: 19487648]

First, MB.; Spitzer, RL.; Gibbon, M.; Williams, JBW. Structured Clinical Interview for DSM-IV Axis I Disorders (SCID) Version 2.0. New York, NY: Biometrics Research Department, New York State Psychiatric Institute; 1998.

Grady C, Haxby J, Horwitz B, Sundaram M, Berg G, Schapiro M, Friedland RP, Rapoport SI. Longitudinal study of the early neuropsychological and cerebral metabolic changes in dementia of the Alzheimer type. Journal of Clinical and Experimental Neuropsychology. 1988; 10:576–596. [PubMed: 3265710]

Grunfeld C, Delaney JA, Wanke C, Currier JS, Scherzer R, Biggs ML, Tien PC, Shlipak MG, Sidney S, Polak JF, O'Leary D, Bacchetti P, Kronmal RA. Preclinical atherosclerosis due to HIV infection: carotid intima-medial thickness measurements from the FRAM study. Aids. 2009; 23:1841–1849. [PubMed: 19455012]

Heaton RK, Franklin DR, Ellis RJ, McCutchan JA, Letendre SL, Leblanc S, Corkran SH, Duarte NA, Clifford DB, Woods SP, Collier AC, Marra CM, Morgello S, Mindt MR, Taylor MJ, Marcotte TD, Atkinson JH, Wolfson T, Gelman BB, McArthur JC, Simpson DM, Abramson I, Gamst A, Fennema-Notestine C, Jernigan TL, Wong J, Grant I. HIV-associated neurocognitive disorders before and during the era of combination antiretroviral therapy: differences in rates, nature, and predictors. Journal of Neurovirology. 2011; 17:3–16. [PubMed: 21174240]

Hollingshead, AB.; Redlich, FC. Social Class and Mental Illness. New York: John Wiley and Sons; 1958.

Holt JL, Kraft-Terry SD, Chang L. Neuroimaging studies of the aging HIV-1-infected brain. J Neurovirol. 2012; 18:291–302. [PubMed: 22653528]

Jahanshad N, Valcour VG, Nir TM, Kohannim O, Busovaca E, Nicolas K, Thompson PM. Disrupted brain networks in the aging HIV+ population. Brain Connect. 2012; 2:335–344. [PubMed: 23240599]

Jernigan TL, Archibald SL, Fennema-Notestine C, Taylor MJ, Theilmann RJ, Julaton MD, Notestine RJ, Wolfson T, Letendre SL, Ellis RJ, Heaton RK, Gamst AC, Franklin DR Jr, Clifford DB, Collier AC, Gelman BB, Marra C, McArthur JC, McCutchan JA, Morgello S, Simpson DM, Grant I. Clinical factors related to brain structure in HIV: the CHARTER study. Journal of Neurovirology. 2011; 17:248–257. [PubMed: 21544705]

Justice AC. HIV and aging: time for a new paradigm. Current HIV/AIDS Reports. 2010; 7:69–76. [PubMed: 20425560]

Kallianpur KJ, Kirk GR, Sailasuta N, Valcour V, Shiramizu B, Nakamoto BK, Shikuma C. Regional Cortical Thinning Associated with Detectable Levels of HIV DNA. Cereb Cortex. 2011

Karnofsky, DA. The clinical evaluation of chemotherapeutic agents in cancer. In: MacLeod, CM., editor. Evaluation of Chemotherapeutic Agents. New York: Columbia University Press; 1949. p. 191-205.

Karpiak, SE. The complications of success: The aging HIV population. New York City: AIDS Community Research Initiative of America (ACRIA); 2011.

Kuper M, Rabe K, Esser S, Gizewski ER, Husstedt IW, Maschke M, Obermann M. Structural gray and white matter changes in patients with HIV. J Neurol. 2011; 258:1066–1075. [PubMed: 21207051]

Laird NM, Ware JH. Random-effects models for longitudinal data. Biometrics. 1982; 38:963–974. [PubMed: 7168798]

Letendre S, Marquie-Beck J, Capparelli E, Best B, Clifford D, Collier AC, Gelman BB, McArthur JC, McCutchan JA, Morgello S, Simpson D, Grant I, Ellis RJ. Validation of the CNS Penetration-Effectiveness rank for quantifying antiretroviral penetration into the central nervous system. Archives of Neurology. 2008; 65:65–70. [PubMed: 18195140]

Letendre SL, Ellis RJ, Ances BM, McCutchan JA. Neurologic complications of HIV disease and their treatment. Top HIV Med. 2010; 18:45–55. [PubMed: 20516524]

Likar B, Viergever MA, Pernus F. Retrospective correction of MR intensity inhomogeneity by information minimization. EEE Transactions on Medical Imaging. 2001; 20:1398–1410.

Luther VP, Wilkin AM. HIV infection in older adults. Clinics in Geriatric Medicine. 2007; 23:567–583. vii. [PubMed: 17631234]

Mathalon DH, Sullivan EV, Rawles JM, Pfefferbaum A. Correction for head size in brain-imaging measurements. Psychiatry Research: Neuroimaging. 1993; 50:121–139.

Nelson, HE. The National Adult Reading Test (NART). Windsor, Canada: Nelson Publishing Company; 1982.

Nir TM, Jahanshad N, Busovaca E, Wendelken L, Nicolas K, Thompson PM, Valcour VG. Mapping white matter integrity in elderly people with HIV. Hum Brain Mapp. 2013

Paul RH, Ernst T, Brickman AM, Yiannoutsos CT, Tate DF, Cohen RA, Navia BA. Relative sensitivity of magnetic resonance spectroscopy and quantitative magnetic resonance imaging to cognitive function among nondemented individuals infected with HIV. Journal of the International Neuropsychological Society. 2008; 14:725–733. [PubMed: 18764968]

Pfefferbaum A, Lim KO, Zipursky RB, Mathalon DH, Rosenbloom MJ, Lane B, Ha CN, Sullivan EV. Brain gray and white matter volume loss accelerates with aging in chronic alcoholics: A quantitative MRI study. Alcoholism: Clinical and Experimental Research. 1992; 16:1078–1089.

Pfefferbaum A, Mathalon DH, Sullivan EV, Rawles JM, Zipursky RB, Lim KO. A quantitative magnetic resonance imaging study of changes in brain morphology from infancy to late adulthood. Archives of Neurology. 1994; 51:874–887. [PubMed: 8080387]

Pfefferbaum A, Rohlfing T, Rosenbloom MJ, Chu W, Colrain IM, Sullivan EV. Variation in longitudinal trajectories of regional brain volumes of healthy men and women (ages 10 to 85 years) measured with atlas-based parcellation of MRI. NeuroImage. 2013; 65:176–193. [PubMed: 23063452]

Pfefferbaum A, Rosenbloom MJ, Rohlfing T, Adalsteinsson E, Kemper CA, Deresinski S, Sullivan EV. Contribution of alcoholism to brain dysmorphology in HIV infection: Effects on the ventricles and corpus callosum. NeuroImage. 2006; 33:239–251. [PubMed: 16877010]

Pfefferbaum A, Rosenbloom MJ, Sassoon SA, Kemper CA, Deresinski S, Rohlfing T, Sullivan EV. Regional brain structural dysmorphology in human immunodeficiency virus infection: Effects of acquired immune deficiency syndrome, alcoholism, and age. Biological Psychiatry. 2012; 72:361–370. [PubMed: 22458948]

Ragin AB, D'Souza G, Reynolds S, Miller E, Sacktor N, Selnes OA, Martin E, Visscher BR, Becker JT. Platelet decline as a predictor of brain injury in HIV infection. J Neurovirol. 2011; 17:487–495. [PubMed: 21956288]

Raz N, Ghisletta P, Rodrigue KM, Kennedy KM, Lindenberger U. Trajectories of brain aging in middle-aged and older adults: regional and individual differences. NeuroImage. 2010; 51:501–511. [PubMed: 20298790]

Resnick SM, Pham DL, Kraut MA, Zonderman AB, Davatzikos C. Longitudinal magnetic resonance imaging studies of older adults: a shrinking brain. Journal of Neuroscience. 2003; 23:3295–3301. [PubMed: 12716936]

Rogosa D, Brandt D, Zimowski M. A growth curve approach to the measurement of change. Psychological Bulletin. 1982; 92:727–748.

Rohlfing T, Maurer CR. Nonrigid image registration in shared-memory multiprocessor environments with application to brains, breasts, and bees. IEEE Transactions on Information Technology in Biomedicine. 2003; 7:16–25. [PubMed: 12670015]

Rohlfing T, Maurer CRJ. Shape-based averaging for combination of multiple segmentations. Med Image Comput Comput Assist Interv Int Conf Med Image Comput Comput Assist Interv. 2005; 8:838–845.

Rohlfing T, Zahr NM, Sullivan EV, Pfefferbaum A. The SRI24 multi-channel atlas of normal adult human brain structure. Human Brain Mapping. 2010; 31:798–819. [PubMed: 20017133]

Sacktor N, Skolasky R, Selnes OA, Watters M, Poff P, Shiramizu B, Shikuma C, Valcour V. Neuropsychological test profile differences between young and old human immunodeficiency virus-positive individuals. J Neurovirol. 2007; 13:203–209. [PubMed: 17613710]

Scott JC, Woods SP, Carey CL, Weber E, Bondi MW, Grant I. Neurocognitive consequences of HIV infection in older adults: an evaluation of the "cortical" hypothesis. AIDS Behav. 2011; 15:1187–1196. [PubMed: 20865313]

Smith S. Fast robust automated brain extraction. Human Brain Mapping. 2002; 17:143–155. [PubMed: 12391568]

Spudich SS, Ances BM. Neurologic complications of HIV infection. Top Antivir Med. 2012; 20:41–47. [PubMed: 22710906]

Stout J, Ellis R, Jernigan T, Archibald S, Abramson I, Wolfson T, McCutchan J, Wallace M, Atkinson J, Grant I. Progressive cerebral volume loss in human immunodeficiency virus infection: a longitudinal volumetric magnetic resonance imaging study. Archives of Neurology. 1998; 55:161–168. [PubMed: 9482357]

Sullivan EV, Pfefferbaum A, Rohlfing T, Baker FC, Padilla ML, Colrain IM. Developmental change in regional brain structure over 7 months in early adolescence: Comparison of approaches for longitudinal atlas-based parcellation. NeuroImage. 2011a; 57:214–224. [PubMed: 21511039]

Sullivan EV, Rosenbloom MJ, Rohlfing T, Kemper CA, Deresinski S, Pfefferbaum A. Pontocerebellar contribution to ataxia and psychomotor slowing in HIV infection without dementia. Brain Imaging and Behavior. 2011b; 5:12–24. [PubMed: 20872291]

Taki Y, Kinomura S, Sato K, Goto R, Kawashima R, Fukuda H. A longitudinal study of gray matter volume decline with age and modifying factors. Neurobiology of Aging. 2011; 32:907–915. [PubMed: 19497638]

Thomas JB, Brier MR, Snyder AZ, Vaida FF, Ances BM. Pathways to neurodegeneration: effects of HIV and aging on resting-state functional connectivity. Neurology. 2013; 80:1186–1193. [PubMed: 23446675]

Thompson PM, Dutton RA, Hayashi KM, Lu A, Lee SE, Lee JY, Lopez OL, Aizenstein HJ, Toga AW, Becker JT. 3D mapping of ventricular and corpus callosum abnormalities in HIV/AIDS. NeuroImage. 2006; 31:12–23. [PubMed: 16427319]

Thompson PM, Dutton RA, Hayashi KM, Toga AW, Lopez OL, Aizenstein HJ, Becker JT. Thinning of the cerebral cortex visualized in HIV/AIDS reflects CD4+ T lymphocyte decline. Proceedings of the National Academy of Sciences of the United States of America. 2005; 102:15647–15652. [PubMed: 16227428]

Valcour V, Paul R, Neuhaus J, Shikuma C. The Effects of Age and HIV on Neuropsychological Performance. J Int Neuropsychol Soc. 2011; 17:190–195. [PubMed: 21144102]

Valcour V, Yee P, Williams AE, Shiramizu B, Watters M, Selnes O, Paul R, Shikuma C, Sacktor N. Lowest ever CD4 lymphocyte count (CD4 nadir) as a predictor of current cognitive and neurological status in human immunodeficiency virus type 1 infection--The Hawaii Aging with HIV Cohort. J Neurovirol. 2006; 12:387–391. [PubMed: 17065131]

van Vonderen MG, Lips P, van Agtmael MA, Hassink EA, Brinkman K, Geerlings SE, Sutinen J, Ristola M, Danner SA, Reiss P. First line zidovudine/lamivudine/lopinavir/ritonavir leads to greater bone loss compared to nevirapine/lopinavir/ritonavir. Aids. 2009; 23:1367–1376. [PubMed: 19424051]

Zhang Y, Brady M, Smith S. Segmentation of brain MR images through a hidden Markov random field model and the expectation maximization algorithm. IEEE Transactions Medical Imaging. 2001; 20:45–57.

Figure 1.
Distribution of ages at MRI for each control (black) and each HIV-infected (green) participant.

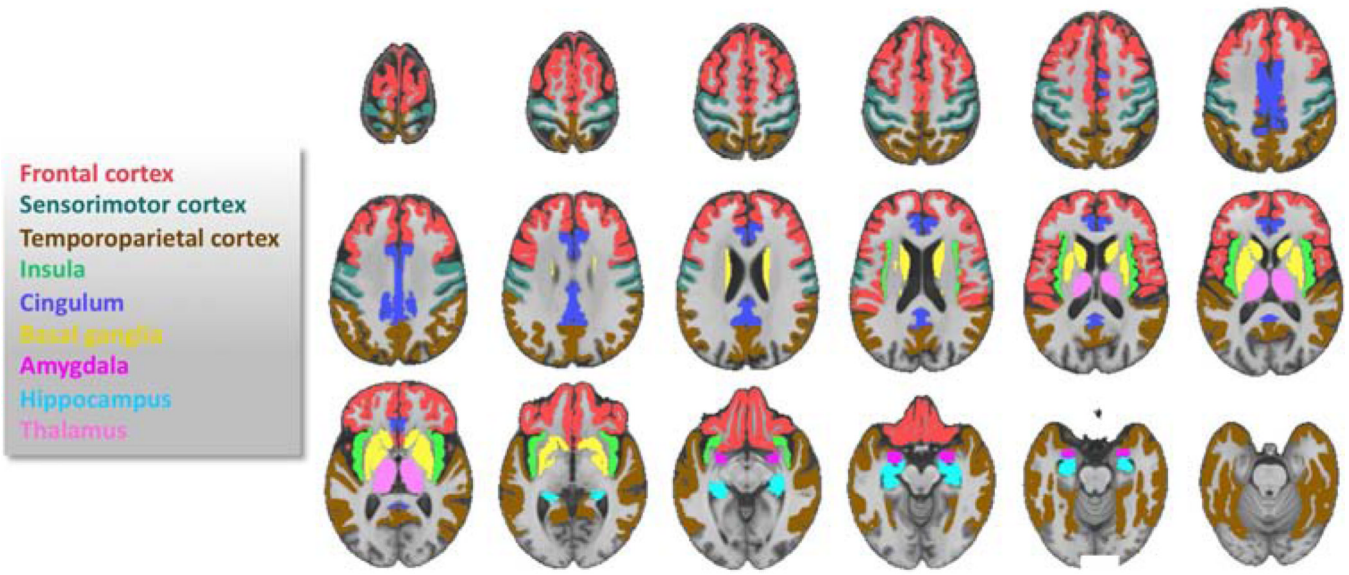

Figure 2.
Color-coded parcellations of MRI superimposed on the SRI24 atlas T1-weighted template image.

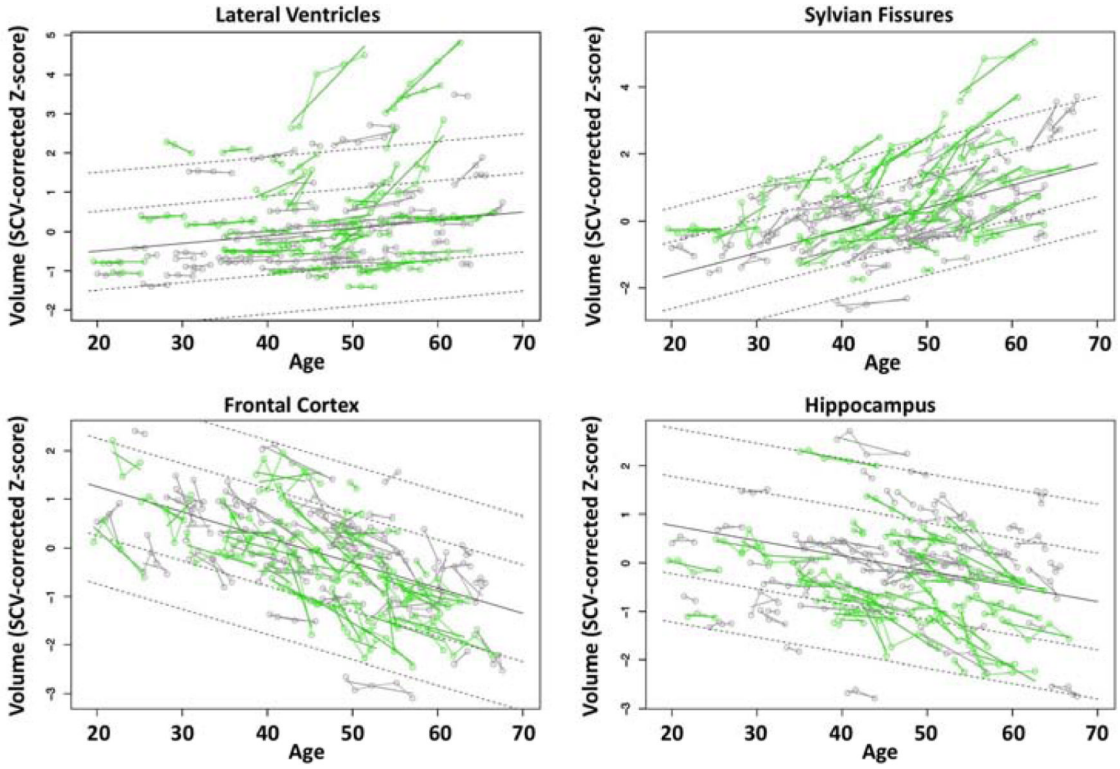

Figure 3.

Plots of individual supratentorial cranial volume (SCV)-corrected Z-scores by age for each control (gray) and each HIV-infected participant (green) for the lateral ventricles, Sylvian fissures, frontal cortex, and hippocampus. Each participant's values are connected over time and the age-centered slope of each participant is overlaid on his or her longitudinal data points. The long solid black regression line is the expected volume by age regression based on the controls; dotted lines are ±1 and 2 S.D.

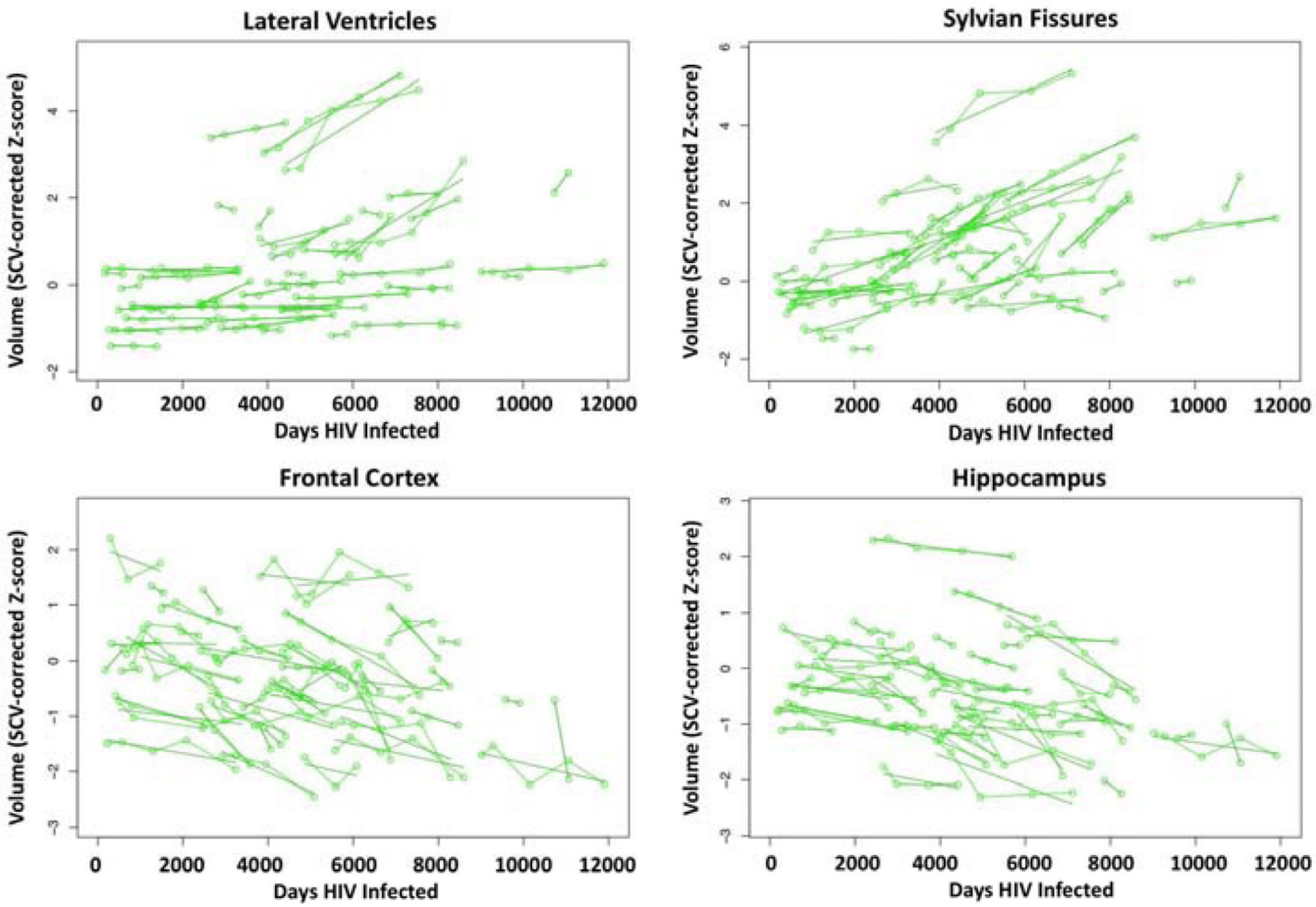

Figure 4.

Plots of individual supratentorial cranial volume (SCV)-corrected Z-scores and overlaid slopes by duration of disease (days of HIV infection) for each HIV-infected participant (green) for the lateral ventricles, Sylvian fissures, frontal cortex, and hippocampus.

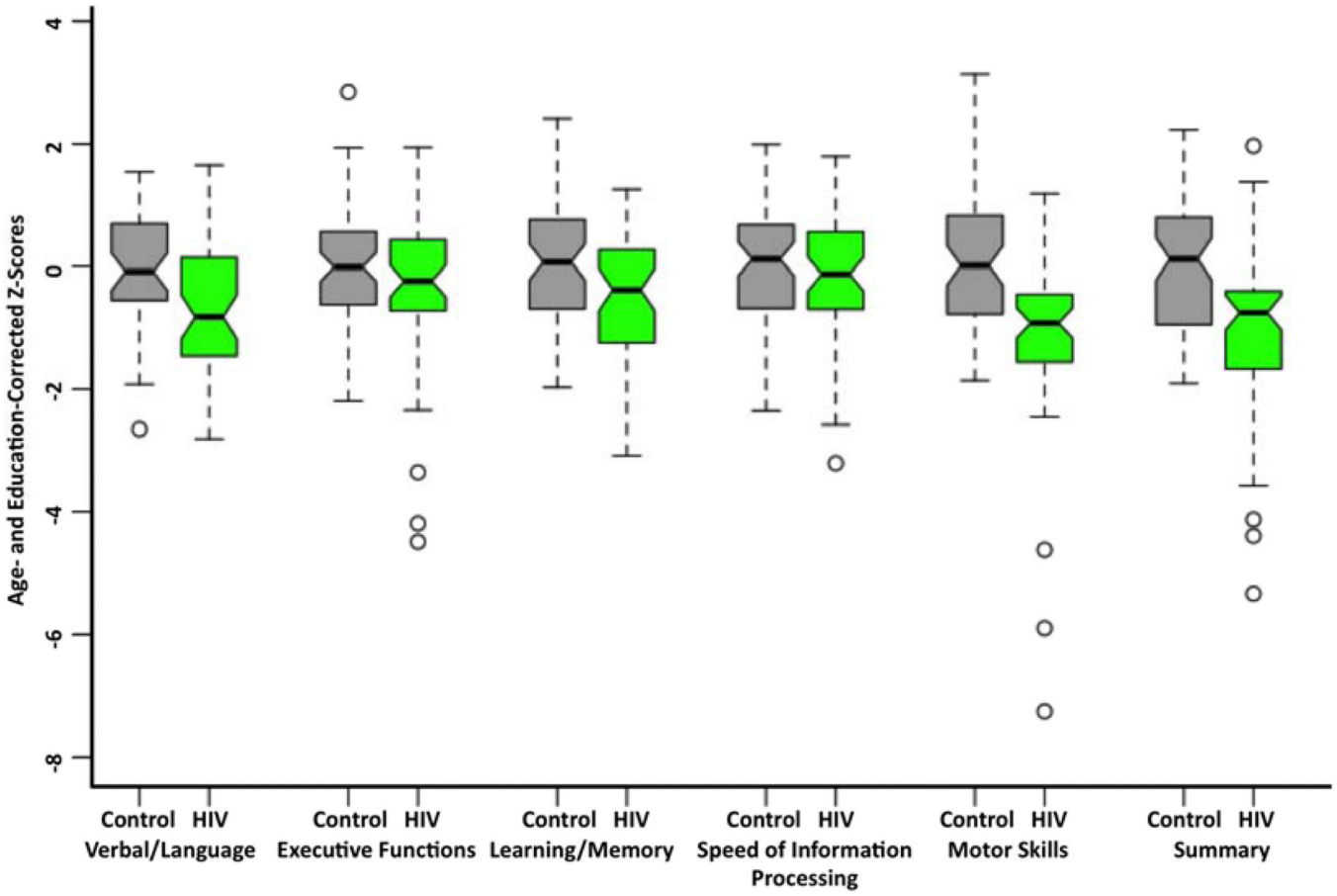

Figure 5.
Box plots of the 5 neuropsychological functional domain and Summary Z-scores for control (gray) and HIV-infected (green) participants.

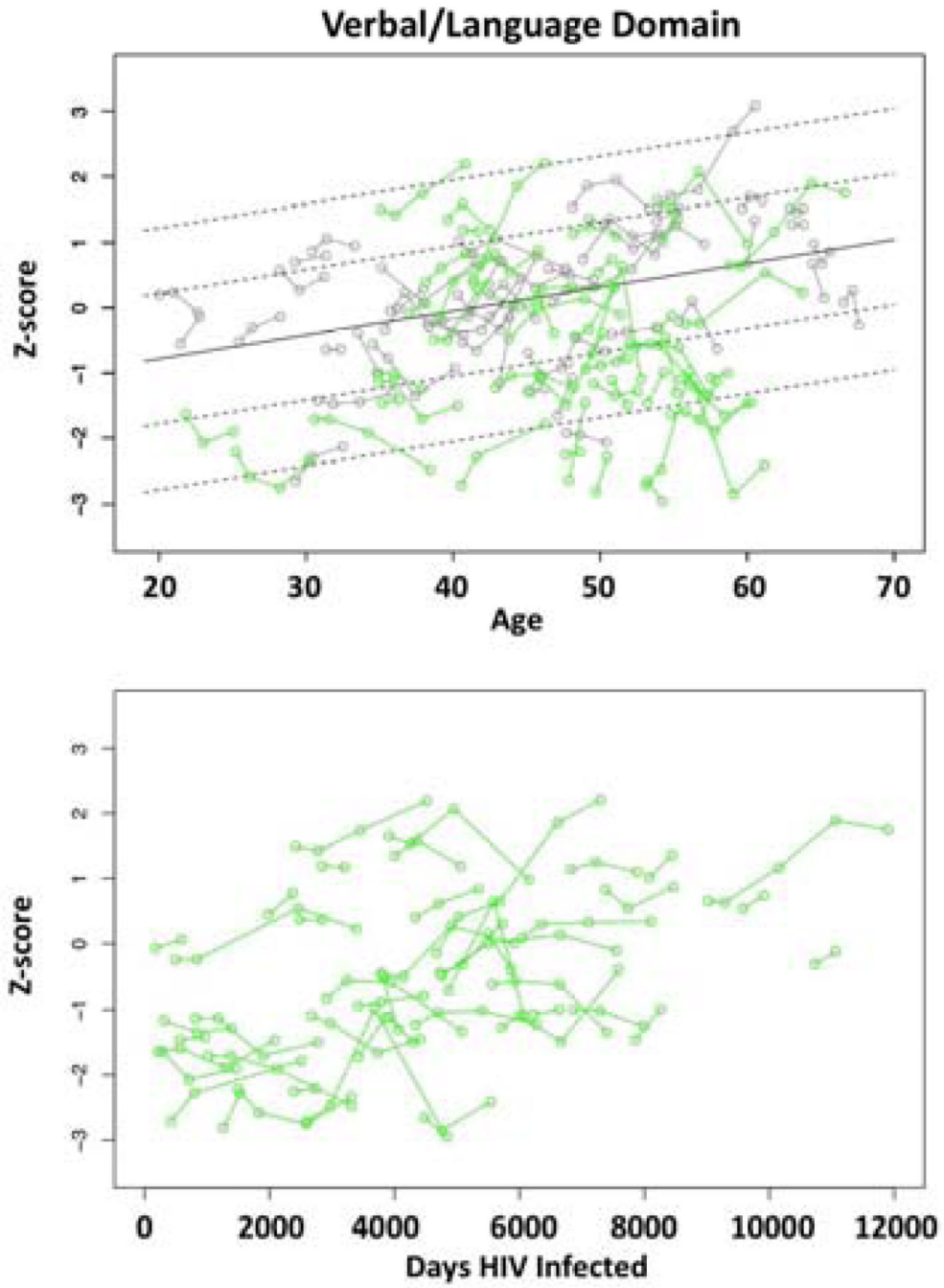

Figure 6.

Top: Plots of individual Verbal/Language domain Z-scores by age for each control (gray) and each HIV-infected participant (green). Solid line is the expected value by age regression based on the controls; dotted lines are ±1 and 2 S.D. Bottom: Plots of individual Verbal/Language domain Z-scores by duration of disease (days of HIV infection) for each HIV-infected participant (green).

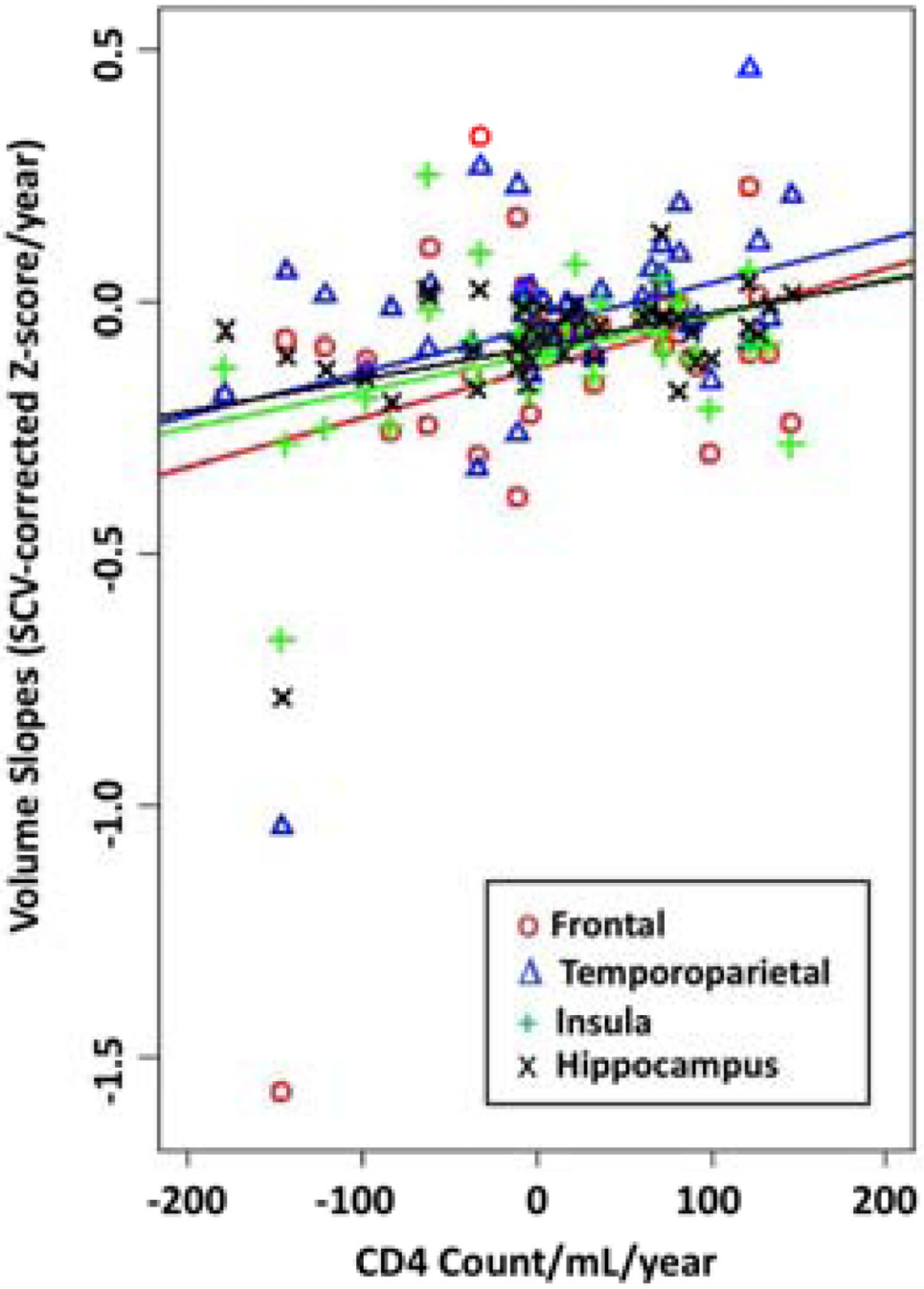

Figure 7.
Plots of slopes of regional volumes as a function of slopes of CD4 count/mL/year. Insula (green), hippocampus (black), temporoparietal cortex (blue), frontal cortex (red). ROI captions are adjacent to the values of one HIV-infected participant with extreme scores.

Table 1

Study groups at each MRI session

	Control (C)	HIV (H)
	Baseline	
Sex: M/F	31/34	34/17
Age: mean	44.7	44.9
SD	(11.4)	(9.4)
	MRI 2	
Sex: M/F	31/34	34/17
Age: mean	46.0	45.9
SD	(11.5)	(9.3)
	MRI 3	
Sex: M/F	20/14	26/12
Age: mean	46.9	46.1
SD	(11.5)	(10.0)
	MRI 4	
Sex: M/F	9/7	12/7
Age: mean	49.3	49.5
SD	(8.0)	(11.1)
	MRI 5	
Sex: M/F	4/3	5/5
Age: mean	53.2	57.2
SD	(6.2)	(8.0)

Table 2

Baseline demographic characteristics of the study groups (N=116): mean (SD) or frequency count

		Control (C)	HIV (H)	Group Differences χ^2 or t-test p-value
Sex: M/F		31/34	34/17	0.0636
Age (yrs)		44.7	44.9	n.s.
		(11.4)	(9.4)	
	n=	65	51	
Education (yrs)		15.4	13.4	0.0002
		(2.5)	(3.0)	
	n=	65	51	
Handedness score		23.2	24.2	n.s.
(**RH=14–30; LH=50–70**)		(12.5)	(9.8)	
	n=	63	51	
Body mass index		26.1	26.1	n.s.
		(5.2)	(4.2)	
	n=	65	51	
Socioeconomic status		30.4	38.3	0.0039
(**lower score=higher status**)		(13.1)	(15.0)	
	n=	58	51	
NART IQ		111.8	106.5	0.0016
		(7.2)	(9.6)	
	n=	61	44	
Beck Depression Inventory II		2.3	12.2	0.0001
		(3.3)	(9.0)	
	n=	38	47	
Global Assessment of Functioning (GAF)		82.0	70.6	0.0001
		(7.8)	(11.0)	
	n=	37	51	
HIV onset age (years)		—	34.5	—
			(9.0)	
	n=		49	
HIV duration (days)		—	3908.0	—
			(2655.0)	
	n=		49	
CD4 cell count (100/mm^3)		—	515.5	—
			(268.0)	
	n=		51	
CD4 cell count nadir (100/mm^3)		—	193.8	—
			(145.4)	
	n=		42	
Viral load		—	9608.9	—
			(20664.0)	

		Control (C)	HIV (H)	Group Differences χ^2 or t-test p-value
	n=		51	
AIDS-defining event (no/yes)		—	26/25	—
Hepatitis C virus (positive/negative)		—	14/37	—
	n=		51	
ART or HAART (yes/no)		—	41/10	—
	n=		51	
Smoker (never/current or past)		29/10	20/28	0.0045
	n=	39	48	
Self-Defined Ethnicity				
Caucasian		41	29	n.s.
African American		12	20	0.023
Other		12	2	n.s.

Table 3

Group differences in level and slope of trajectories

	A. Volume differences		B. Trajectory differences		C. Acceleration (slope) with age	
ROI	**t**	**p**	**t**	**p**	**t**	**p**
Lateral ventricles	1.3111	0.1925	2.5715	0.0108	1.7101	0.0900
Sylvian fissures	2.1708	0.0320	1.7452	0.0823	1.4851	0.1403
Frontal cortex	−1.4266	0.1565	−1.0916	0.2761	−2.5370	0.0126
Sensorimotor cortex	−0.2914	0.7713	0.1812	0.8563	−2.3352	0.0213
Temporoparietal cortex	−1.8728	0.0637	−0.7269	0.4680	−2.2728	0.0250
Cingulum	−2.0626	0.0414	−0.9936	0.3214	−1.3730	0.1725
Insula	−3.3542	0.0011	−1.9828	0.0486	−1.8737	0.0636
Thalamus	−3.6202	0.0004	−1.6656	0.0972	−2.6255	0.0099
Hippocampus	−2.4597	0.0154	−2.8136	0.0053	−0.8254	0.4109
Amygdala	−1.3382	0.1835	−0.5882	0.5570	0.6580	0.5119
Basal ganglia	−0.6206	0.5361	0.4741	0.6359	−0.5426	0.5885

Table 4

MRI volumes and trajectories as functions of duration of disease and age

	A. Volume		B. Trajectory	
ROI	**t**	**p**	**t**	**p**
Lateral ventricles	2.3985	0.0205	2.1670	0.0324
Sylvian fissures	3.2965	0.0019	1.5586	0.1220
Frontal cortex	−2.0742	0.0436	−0.6189	0.5373
Sensorimotor cortex	−2.8402	0.0066	−1.3943	0.1661
Temporoparietal cortex	−1.5168	0.1360	−2.1733	0.0319
Cingulum	−1.1724	0.2470	−0.1055	0.9162
Insula	−1.0160	0.3148	−0.9870	0.3259
Thalamus	−2.0557	0.0454	−2.0091	0.0470
Hippocampus	−2.1765	0.0346	−1.5996	0.1126
Amygdala	0.4059	0.6866	−0.1269	0.8992
Basal ganglia	−0.9534	0.3453	−1.0166	0.3116

	C. Multiple Regression					
	Duration		Age			
ROI	**t**	**p**	**t**	**p**	**F(2,46)**	**p**
Lateral ventricles	1.7220	0.0918	0.6340	0.5289	2.5930	0.0857
Sylvian fissures	2.3920	0.0209	0.2760	0.7837	3.8460	0.0286
Frontal cortex	−2.7600	0.0083	0.0290	0.9768	4.5730	0.0154
Sensorimotor cortex	−1.3930	0.1700	−1.5010	0.1400	3.5960	0.0354
Temporoparietal cortex	−2.5780	0.0132	−0.4470	0.6568	4.7310	0.0135
Cingulum	−2.8120	0.0072	1.2380	0.2220	3.9560	0.0260
Insula	−2.4000	0.0205	0.6570	0.5145	2.9520	0.0622
Thalamus	−0.4770	0.6355	−2.7930	0.0076	5.5350	0.0070
Hippocampus	−2.7500	0.0085	−0.3690	0.7141	5.1750	0.0094
Amygdala	−0.3550	0.7240	−0.2450	0.8080	0.1565	0.8556
Basal ganglia	−1.7670	0.0839	−0.4140	0.6805	2.3650	0.1053

Table 5

Group trajectory differences in neuropsychological composite scores

	A. Performance differences		B. Trajectory differences		C. Acceleration (slope) with age	
Composite Score	**t**	**p**	**t**	**p**	**t**	**p**
Verbal/Language	−3.2481	0.0016	0.0521	0.9585	0.1646	0.8696
Executive Functions	−2.4255	0.0169	−2.5153	0.0126	0.5984	0.5509
Learning/Memory	−2.7408	0.0072	−1.3411	0.1815	−0.2005	0.8415
Speed of Information	−1.7251	0.0874	−1.9287	0.0551	0.6081	0.5444
Motor Skills	−4.8651	0.0000	1.5593	0.1204	0.4420	0.6594
Total	−4.2696	0.0000	−2.6188	0.0094	0.6383	0.5247

Table 6

Performance composite trajectories related to duration of disease

	A. Performance differences		B. Trajectory differences		C. Rate of change with disease duration		
Composite Score	**t**	**p**	**t**	**p**	**r**	**t**	**p**
Verbal/Language	3.2387	0.0023	1.1846	0.2388	0.0157	−0.1026	0.9188
Executive Functions	1.1937	0.2390	0.8957	0.3726	0.0694	0.4507	0.6545
Learning/Memory	2.0223	0.0492	0.8399	0.4032	0.0430	0.2787	0.7818
Speed of Information	2.6558	0.0110	0.9810	0.3290	0.0570	−0.3787	0.7067
Motor Skills	0.3171	0.7527	−0.0625	0.9503	0.0962	−0.6408	0.5250
Total	2.4495	0.0184	0.9599	0.3394	0.0725	−0.4820	0.6322

Table 7

MRI slopes correlated with CD4 slopes in the HIV-infected group

ROI	r	p	Rho	p
Lateral ventricles	−0.4435	0.0020	−0.2649	0.0755
Sylvian fissures	−0.5260	0.0002	−0.3875	0.0082
Frontal cortex	0.3816	0.0089	0.2990	0.0439
Sensorimotor cortex	0.4499	0.0017	0.2073	0.1665
Temporoparietal cortex	0.4148	0.0042	0.3399	0.0213
Cingulum	0.4148	0.0042	0.2475	0.0973
Insula	0.4887	0.0006	0.3226	0.0292
Thalamus	−0.1359	0.3680	−0.1517	0.3133
Hippocampus	0.4885	0.0006	0.4350	0.0028
Amygdala	0.1761	0.2417	0.0404	0.7893
Basal ganglia	−0.0047	0.9752	−0.0157	0.9174

Table 8

Multiple regression: MRI trajectories as functions of CD4 count slopes and age

	Mean age		CD4 slope		
ROI	**t**	**p**	**t**	**p**	**F (df=2,43)**
Lateral ventricles	1.075	0.288	**−3.013**	**0.004**	5.983
Sylvian fissures	0.592	0.557	**−3.877**	**0.000**	8.466
Frontal cortex	−0.957	0.344	**2.495**	**0.017**	4.201
Sensorimotor cortex	−1.557	0.127	**3.024**	**0.004**	6.976
Temporoparietal cortex	−1.496	0.142	**2.713**	**0.010**	5.820
Cingulum	0.410	0.684	**3.018**	**0.004**	4.570
Insula	−0.048	0.962	**3.592**	**0.001**	6.747
Thalamus	**−3.337**	**0.002**	−1.644	0.107	6.077
Hippocampus	−1.441	0.157	**3.403**	**0.001**	8.103
Amygdala	−0.193	0.848	1.113	0.272	0.707
Basal ganglia	−1.463	0.151	−0.318	0.752	1.071

Table 9

Trajectories of uncorrected ROI slopes showing change in cc/year in control and HIV-infected groups

	Control Group				HIV-infected Group			
ROI	**Mean**	**Min**	**Max**	**% change**	**Mean**	**Min**	**Max**	**% change**
Lateral ventricles	0.039	−0.560	1.539	0.167	0.378	−0.839	3.801	1.892
Sylvian fissures	0.101	−0.363	0.575	2.312	0.208	−0.485	1.271	3.769
Frontal cortex	−1.331	−8.494	6.094	−0.759	−1.718	−19.544	4.141	−1.042
Sensorimotor cortex	−0.204	−2.244	1.157	−0.591	−0.226	−4.546	1.557	−0.733
Temporoparietal cortex	−0.782	−8.015	8.019	−0.426	−0.650	−13.944	6.127	−0.390
Cingulum	−0.199	−0.950	0.412	−0.749	−0.276	−1.945	0.293	−1.086
Insula	−0.112	−0.771	0.342	−0.687	−0.170	−0.965	0.439	−1.109
Thalamus	−0.033	−0.219	0.122	−0.218	−0.037	−0.190	0.139	−0.264
Hippocampus	−0.032	−0.210	0.196	−0.314	−0.069	−0.597	0.205	−0.727
Amygdala	−0.007	−0.062	0.093	−0.221	−0.008	−0.132	0.081	−0.243
Basal ganglia	−0.083	−0.532	0.195	−0.416	−0.075	−0.401	0.186	−0.392